High-order harmonic generation processes in classical and quantum anharmonic oscillators

Balcou, P; L'Huillier, Anne; Escande, D

Published in:
Physical Review A (Atomic, Molecular and Optical Physics)

DOI:
10.1103/PhysRevA.53.3456

1996

High-order harmonic generation processes in classical and quantum anharmonic oscillators

Ph. Balcou,[1,2] Anne L'Huillier,[2,3] and D. Escande[4,5]

[1]*Laboratoire d'Electronique Quantique-Physique des Lasers, Unité Associée 1202, Centre National de la Recherche Scientifique, Université de Rennes 1, Campus de Beaulieu, F-35042 Rennes, France*

[2]*Service des Photons, Atomes et Molécules, Bâtiment 522, Centre d'Etudes de Saclay, Commissariat à l'Energie Atomique, F-91191 Gif-sur-Yvette, France*

[3]*Department of Physics, Lund Institute of Technology, P.O. Box 118, S-221 00 Lund, Sweden*

[4]*Association Euratom–Commissariat à l'Energie Atomique pour la Fusion, Département de Recherche sur la Fusion Contrôlée, Centre d'Etudes de Cadarache, F-13108 St-Paul-lez-Durance, France*

[5]*Equipe Turbulence Plasma, Unité Associée 773, Centre National de la Recherche Scientifique, Université de Provence, Institut Méditérannéen de Technologie, F-13451 Marseille Cedex, France*

(Received 20 July 1995)

We present a theoretical study of high-order harmonic generation by a slowly driven ''Duffing'' anharmonic oscillator. The power spectra are shown to display a plateau of high harmonics, which ends up with a sharp cutoff. The classical dynamics is analyzed with the adiabatic invariance theorem, which yields a simple interpretation to this characteristic behavior. We compare with the quantum case by solving numerically the time-dependent Schrödinger equation, and outline the similarity between classical damping and quantum-mechanical ionization processes. This allows us, in particular, to interpret the existence of intrinsic phases between high harmonics and the driving field. We further discuss the implication of these relaxation processes on the coherence of high harmonics, as well as the existence of interference processes yielding quasiresonant structures in intensity dependences.

PACS number(s): 32.80 Rm, 42.65 Ky

I. INTRODUCTION

High-order harmonic generation by noble gas atoms interacting with intense laser pulses has become one of the major topics in multiphoton physics. Extremely high orders have been observed [1,2], thus demonstrating the possibility to generate coherent light pulses in the extreme ultraviolet (XUV) spectral region, with photon energies up to 160 eV. High-order harmonic generation can be used as compact and versatile XUV sources, of interest for instance in atomic and molecular spectroscopy [3]. Recent experimental studies have measured the characteristics of the harmonic beams: angular distributions have been obtained by Peatross and Meyerhofer [5], Tisch *et al.* [4], and Salières *et al.* [6]; temporal [7] and spectral profile measurements [8] have also been reported.

The theory of these highly nonlinear processes has been extensively developed over the past few years, to investigate both the single-atom response, and propagation and phase-matching phenomena [9]. Several methods have been used to describe the atomic response. Most prominent among these are the integration of the time-dependent Schrödinger equation (TDSE) for an atom in the single active electron approximation [10,11], and the solution of the coupled time-independent Floquet equations for hydrogen [12]. A number of simplified models have also been successfully considered, such as one-dimensional approximations in a soft-Coulomb potential [13,14], the integration of the equations of motion for a classical hydrogen system [15], and even cruder models such as a two-level system in a strong field [16–19].

The harmonic distribution presents a characteristic shape, consisting of a decrease for the first orders, followed by a long plateau which ends up with a rather sharp cutoff. Numerical calculations of Krause *et al.* [20]. have shown that the single-atom cutoff, expressed in terms of photon energy, scales as I_p+3U_p, where I_p is the atomic ionization potential, and U_p is the ponderomotive potential, equal to the average quiver energy of a free electron in the field. This scaling is valid in a strong-field and low-frequency limit such that ionization takes place by a tunneling mechanism ($\sqrt{I_p/2U_p}<1$). This was later explained by Kulander, Schafer, and Krause [21] and Corkum [22], in a two-step semiclassical model. Lewenstein and co-workers [23,24] subsequently recovered the same cutoff law and interpretation in a quantum, analytical model, again valid in a strong-field, tunnel-ionization limit. The experimental cutoff law actually depends on complex macroscopic parameters, for example, focusing conditions; taking these effects into account, L'Huillier *et al.* [23] were able to confirm the single-atom I_p+3U_p law. This semi-classical model therefore tends to become a theoretical paradigm for high-order harmonic generation.

It should be pointed out that all model atoms studied so far display the charasteristic response: decrease, plateau, and cutoff. However, they do not necessarily yield the I_p+3U_p cutoff law. For instance, a different cutoff law is predicted in a two-level system, or in a slowly driven classical hydrogen atom. The semiclassical model, while describing successfully the atomic response in a tunneling regime, obviously cannot account for the different scaling laws obtained in other models. In contrast, the characteristic plateau-cutoff behavior seems to be a very common property (model independent) of the response of a nonlinear system strongly driven by a low-frequency force. This apparent universality is not fully understood yet.

The purpose of this paper is to present a detailed analysis

of high-order harmonic generation by an anharmonic oscillator. The quartic anharmonic oscillator, or ''Duffing'' oscillator, seems to be indeed the simplest centrosymmetric nonlinear system, and as such is widely used as an introductive model in nonlinear optics textbooks [25,26]. We have recently pointed out that the power spectrum of a classical anharmonic oscillator, driven by a strong low-frequency force, also displays the typical plateau-cutoff behavior [27].

The anharmonic oscillator presents several appealing properties, which make its study particularly worthy. A considerable amount of literature exists on the nonlinear dynamics of one-dimensional oscillators (see, for instance, Nayfeh and Mook [28]), and on the particular case of time-dependent anharmonic oscillators. A recent review of this field can be found in Bose *et al.* [29].. Powerful methods of analytical Hamiltonian mechanics, such as action-angle representations, can be used to study the motion in this system. These methods allow us to give a simple interpretation of the plateau-cutoff behavior, and to explain particular (and also apparently universal) properties of high-order harmonics, such as the existence of intrinsic phases or of quantum interferences. Moreover, the problem is well suited to a comparison between the classical and quantum-mechanical cases, and, possibly, to propagation studies [5]. Our aim is not to obtain realistic solutions for the single-atom response, and the scaling laws obtained here are due to the specific properties of the anharmonic oscillator Hamiltonian. We wish to show, however, that this very simple model may help to understand some aspects of high-order harmonic generation.

This article is organized as follows. We first study the classical problem of an anharmonic oscillator subjected to a low-frequency driving force. The existence of high-order harmonics of the motion can be interpreted simply by taking advantage of the adiabatic invariance theorem. We emphasize the role of a small damping term in obtaining periodic solutions. We then discuss the relevance of this problem to the quantum-mechanical case, and proceed to study the quantum-mechanical dynamics, by solving numerically the time-dependent Schrödinger equation. We outline in particular the importance of ionization as an analog to the classical damping force. The last part of this paper is devoted to the investigation, within the anharmonic oscillator model, of three puzzling properties of high-order harmonics. We first address the problem of the intrinsic phases of high-order harmonics relative to the driving field, which recently aroused much interest because of their incidence on propagation effects. We then proceed to show how dynamical interference effects arise in the model, and result in broad resonantlike structures in the intensity dependences of high harmonics. We emphasize a coherence problem for high harmonics, related to the existence of ''hyper-Raman'' peaks. We point out that high-order harmonic generation is a dynamical process, which does not follow instantaneously the variations of the forcing field. We discuss the relevant time scales, and show that in most cases, the coherence of the harmonics is maintained thanks to the ionization process.

II. DYNAMICS OF A DRIVEN CLASSICAL ANHARMONIC OSCILLATOR

We first study the motion of a classical ''electron'' in a quartic confining anharmonic potential (Duffing oscillator), submitted to a strong low-frequency force $E(t)=E_0\sin(\omega t)$. The potential can be written as

$$V(x)=\frac{\omega_0^2}{2}x^2+\frac{v}{4}x^4, \tag{1}$$

and corresponds to the sum of a harmonic oscillator potential, of characteristic frequency ω_0, and an anharmonic term, $vx^4/4$. We chose to study only the confining case $v>0$. Indeed, we are interested in using very strong forcing fields E_0, for which all trajectories ionize almost instantaneously in the case $v<0$. The ratio ω/ω_0 is considered to be of the order of 1/10–1/20, corresponding to the typical ratio between the photon energy of a low-frequency terawatt laser (neodymium glass or titanium sapphire), and the ionization potential of a noble gas.

The equation of motion is

$$\ddot{x}+\Gamma\dot{x}+\omega_0^2x+vx^3=E_0\sin(\omega t). \tag{2}$$

We have considered here a damping term $\Gamma\dot{x}$, whose role will be analyzed later. The parameters used (Γ, ω_0, ω, v, and E_0) are actually redundant. We can therefore rescale the time unit: $t\rightarrow\omega_0 t$, which is equivalent to setting $\omega_0=1$. We will use in the following these rescaled ''atomic'' units for all parameters.

Equation (2) cannot be solved analytically; the motion actually becomes chaotic when the field strength is increased, through a period-doubling mechanism. It should be stressed, however, that the present study is performed at field strengths lower than the first bifurcation threshold, and therefore in a nonchaotic regime.

In order to investigate the oscillator dynamics, we integrate Eq. (2) numerically; we use standard fourth-order or variable-step Runge-Kutta algorithms. The latter method allows us to get any desired level of numerical accuracy, but requires longer computation times. We assume the ''electron'' to be at rest at the origin at $t=0$; the forcing field is turned on linearly on several periods $T_L=2\pi/\omega$ (optical cycle), and is subsequently held at a fixed value E_0.

Although radiation by a classical electron depends on the acceleration $\ddot{x}(t)$, we shall concentrate in the following on the power spectrum $|\tilde{x}(\omega)|^2$ of the position $x(t)$ (which can be identified here with the dipole moment), thus following the most common convention in high-order harmonic generation studies [9,16].

Figures 1(a) and 1(b) (solid line) present typical spectra obtained for $E_0=10$ and 5, respectively. They display the characteristic behavior of high-order harmonic spectra: a steady decrease for the first orders, followed by a long plateau up to a sharp cutoff. This behavior can be explained by considering the variation of the electron position x as a function of time, which is shown in Fig. 2(a) (solid line): the electron oscillates rapidly around a slowly varying central position. The forcing frequency ω is much smaller than the atomic frequency. We can therefore distinguish two time scales, one associated with the period T_L of the low-frequency forcing field, and the other with a period T_{at} characteristic of high frequency motion in the potential well. On the latter time scale, the electron can be seen as freely oscillating in a frozen potential:

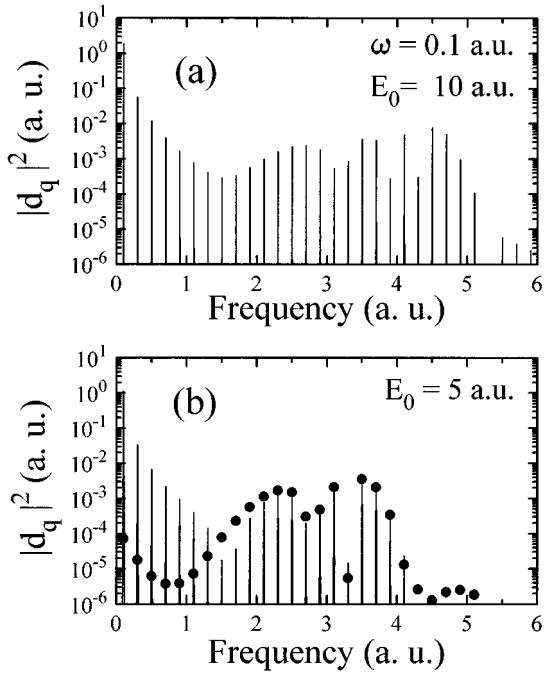

FIG. 1. (a) Typical high-order harmonic spectrum from a classical Duffing anharmonic oscillator. The parameters used are $\omega=0.1$, $v=5$, $E_0=10$, $\Gamma=10$. We use throughout rescaled "atomic" units (a.u.) (i.e., atomic units divided by the oscillator frequency ω_0). (b) Comparison between the full harmonic spectrum obtained for $E_0=5$ (solid line), and that of the high-frequency displacement δx (full dots), responsible for the harmonic plateau [see Eq. (6)].

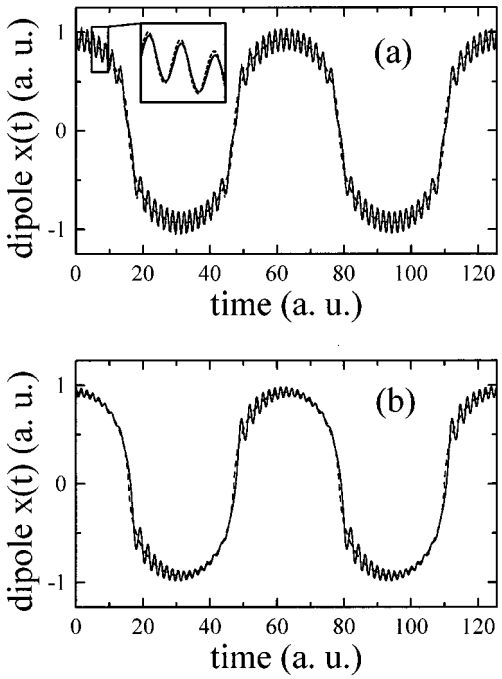

FIG. 2. Time dependence of the electron trajectory (solid line) and of the bottom of the time-dependent potential well (dashes), (a) for weak damping ($\Gamma=0.01$) and (b) for strong damping ($\Gamma=0.15>\omega$). The other parameters correspond to those of Fig. 1(b). The inset shows the difference between the numerical results (solid line) and the analytical results of Eq. (20) (short-dashed line).

$$V'=V-\tilde{E}\,x\,, \tag{3}$$

with $\tilde{E}=E_0\sin(\omega t)$. The average of the quiver motion can be identified with the motion of the bottom of the instantaneous potential well, represented by the dashed line in Fig. 2(a). Let us call x_0 the point representing the bottom of the potential well, which obeys

$$x_0+vx_0^3=E_0\sin(\omega t), \tag{4}$$

and δx the deviation of the electron position from the bottom of the well:

$$\delta x=x-x_0\,. \tag{5}$$

The equation of motion for δx is

$$\begin{aligned}\delta\ddot{x}+(1+3vx_0^2)\,\delta x+(3vx_0\delta x^2+v\,\delta x^3)\\ =(-\ddot{x}_0-\Gamma\dot{x}_0)-\Gamma\,\delta\dot{x}.\end{aligned} \tag{6}$$

The two terms which are nonlinear in δx are of order $\delta x/x_0$ or less, and can therefore be neglected. Let us set $\Omega^2=1+3vx_0^2$. The dominant terms in the left-hand side are of order $\Omega^2\delta x$, while those in the right-hand side are of order $\omega^2\delta x$, with $\omega\ll\Omega$. As a result, we will not consider the right-hand side in a first step, and will focus ourselves on the homogeneous equation

$$\delta\ddot{x}+\Omega^2\delta x=0, \tag{7}$$

which describes a free motion in a slowly varying harmonic potential. This is a Hill equation, well known in the context of celestial mechanics. The electron undergoes a quiver motion in this potential, with an instantaneous frequency Ω. The minimum value of this frequency is $\Omega_{\min}=1$, and the maximum one is $\Omega_{\max}=\sqrt{1+3vx_{\max}^2}$, where $x_{\max}$ is the maximum excursion of the bottom of the potential well. It can be approximated as $x_{\max}\simeq(E_0/v)^{1/3}$ for a strong enough field E_0 [see Eq. (4)]. We have therefore

$$\Omega_{\max}=\sqrt{1+3v^{1/3}E_0^{2/3}}. \tag{8}$$

The Fourier transform (FT) of $x(t)$ can be split into the sum of the FT of $x_0(t)$, whose components regularly decrease with order, and that of $\delta x(t)$, whose components have roughly equal amplitudes between $\Omega_{\min}$ and $\Omega_{\max}$. The overall pattern of the spectrum is therefore interpreted as follows: the steady decrease for the first orders corresponds to the Fourier spectrum of the bottom of the potential well; the plateau is related to the electron motion in this time-dependent well, at shifted atomic frequencies; the cutoff basically corresponds to the highest such frequency.

Numerical results support this interpretation. The predicted maximum frequencies $\Omega_{\max}$ given by Eq. (8) correspond exactly to the numerical results for the cutoff [$\Omega_{\max}\simeq 5$ and 4 in Fig. 1(a) and 1(b), respectively]. Figure 1(b) also enables one to compare directly the power spectra of $x(t)$ and $\delta x(t)$ (full circles). The high-frequency components of $x(t)$ can indeed be identified to the spectrum of $\delta x(t)$, which fits exactly the plateau structure.

One point stays unclear. Why is the ''high-frequency'' motion of $\delta x(t)$ periodic? In fact, the spectrum of $\delta x(t)$ in general includes nonharmonic components, as shown by solving Eq. (7), describing the free motion of δx. The simplest method to obtain an analytical approximation to this equation consists of performing a canonical transformation to use action-angle variables (I,θ). The generating function is

$$F_2(x,\theta,t)=\frac{1}{2}\Omega(t)\,\delta x^2\tan\theta, \tag{9}$$

so that the Hamiltonian $H=(1/2)p_{\delta x}^2+(1/2)\Omega^2(t)\,\delta x^2$ becomes

$$K=I\Omega(t)+\frac{\partial F_2}{\partial t}=I\Omega(t)+\frac{1}{2}\,\delta x^2\tan\theta\Omega'(t). \tag{10}$$

We now take advantage of the quasiadiabaticity of the potential variations: according to the adiabatic theorem, the action I is essentially invariant. Assuming that I is a constant of motion amounts to neglecting the slowly varying term $\partial F_2/\partial t$. The approximate solution in (I,θ) variables is then

$$I=I_0, \tag{11}$$

$$\theta(t)=\theta_0+\int_0^t\Omega(\tau)d\tau, \tag{12}$$

which yields for $\delta x(t)=\sqrt{2I/\Omega}\cos\theta$ the following expression:

$$\delta x(t)=\frac{\sqrt{2I}}{\sqrt{\Omega(t)}}\cos\left(\theta_0+\int_0^t\Omega(\tau)d\tau\right). \tag{13}$$

Although $\Omega(t)$ is periodic, $\cos(\int\Omega)$ is not. Its frequency spectrum displays high-frequency peaks, but at frequencies different from the harmonic ones. Where does the obvious periodicity shown in Figs. 1 and 2 come from?

Numerical studies help in giving the answer to this question. First, we solve Eq. (2) in the conditions of Fig. 1(a) ($v=5$, $E_0=10$), but without damping ($\Gamma=0$). The field is switched on fully adiabatically, by means of a long and smooth ramp, before a constant field period, on which the Fourier analysis is performed. The result is shown in Fig. 3. As previously, the low-frequency part of the spectrum is composed of decreasing harmonic peaks. However, the high-frequency motion is only quasiperiodic; in addition to the high-frequency harmonic peaks, the spectrum shows other series of peaks separated by 2ω. Note that numerical problems may occur here: the fourth-order Runge-Kutta algorithm, which does not intrinsically conserve action, may lead to numerical artifacts, and in particular to an artificial periodicity. All our numerical results show nonharmonic (also called ''hyper-Raman'') peaks. In contrast to some other studies [17], using extremely long ramp durations actually results in increased spurious peaks and noise.

In contrast, the introduction of even a very small damping forces the motion to converge to a periodic solution. This can

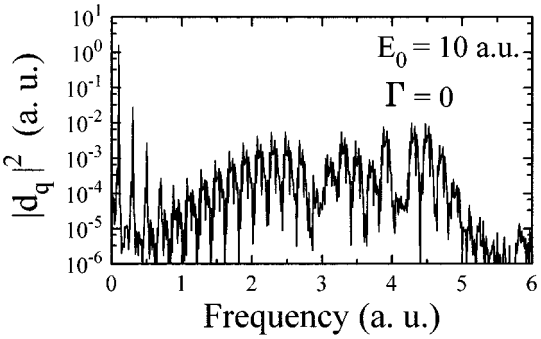

FIG. 3. Spectrum obtained from an undamped harmonic oscillator [same conditions as Fig. 1(a), except for $\Gamma=0$]. The field is switched on quasiadiabatically during 24 optical cycles by a $\sin^2$ ramp.

be explained by considering again Eq. (6) for δx. Its right-hand side includes a damping term $-\Gamma\,\delta\dot{x}$, and a driving term

$$\varphi(t)=-\ddot{x}_0-\Gamma\dot{x}_0, \tag{14}$$

which can be interpreted as the sum of an inertia force, and of damping of the low-frequency motion, acting as a force on the high-frequency motion.

To obtain an analytical expression for δx, we calculate the retarded Green function for

$$\delta\ddot{x}+\Omega^2(t)\,\delta x=\delta(t-\tau), \tag{15}$$

which can easily be shown to be

$$G(\tau,t) \quad =0 \quad \text{for} \quad t<\tau \tag{16}$$

$$G(\tau,t) \quad =\frac{1}{\sqrt{\Omega(\tau)\Omega(t)}}\sin\left(\int_\tau^t\Omega(t')dt'\right) \quad \text{for} \quad t>\tau. \tag{17}$$

In the absence of damping, the solution of Eq. (6) is

$$\delta x(t)=\int_0^t\varphi(\tau)G(\tau,t)d\tau. \tag{18}$$

Damping can be simply introduced by writing the solution as

$$\delta x(t)=\int_0^t\varphi(\tau)G(\tau,t)e^{-\Gamma(t-\tau)/2}d\tau. \tag{19}$$

Moreover, all frequency terms existing in the expression of G should be replaced by $\sqrt{\Omega^2(t)-\Gamma^2/4}$. We shall not write down explicitly this unimportant change. Owing to the existence of damping, the solution depends very little on the initial conditions, which allows us to write the final expression

$$\delta x(t)=\frac{1}{\sqrt{\Omega(t)}}\int_{-\infty}^t\frac{\varphi(\tau)}{\sqrt{\Omega(\tau)}}\sin\left(\int_\tau^t\Omega(t')dt'\right)e^{-\Gamma/2\,(t-\tau)}d\tau. \tag{20}$$

$\delta x(t)$ is now periodic in a steady-state regime. The interpretation is simple: the high-frequency motion consists of periodically driven and damped oscillations in the bottom of the potential well. This behavior can also be observed numerically: Fig. 2(b) shows the variations with time of the dipole $x(t)$, in the same conditions of potential driving field amplitude as in Fig. 2(a), but with a much stronger damping term, such that $\Gamma > \omega$. The quiver motion seems to be excited when the electron trajectory crosses the origin (which corresponds to the maximal value of $\Gamma \dot{x}_0$), and gets rapidly damped, which results in an obvious periodicity for $\delta x(t)$ [30]. A well-known result in Hamiltonian mechanics yields an alternative and more rigorous way to understand this periodicity: a small amount of dissipation always turns stable periodic orbits into attractors, to which the motion relaxes. For larger damping or very strong driving fields, some of these attractors may become strange attractors, and the motion gets chaotic in this system. The accuracy of the approximations used to derive Eqs. (4) and (20) can be checked by comparing the analytical results to the numerical ones. They almost coincide, as shown by the inset in Fig. 2(a).

III. DYNAMICS OF A QUANTUM DRIVEN ANHARMONIC OSCILLATOR

We now come to the study of strongly driven quantum anharmonic oscillators. Our goal is to compare results obtained in the classical and quantum-mechanical cases, and in particular to determine what features of the quantum spectra have an essentially classical origin. It is therefore essential to discuss, first, the nature of the relationship between the two systems.

As far as we are aware, classical mechanics have been used in two different ways to get insights into the dynamics of strongly driven quantum systems. The first method has been developed by Percival and co-workers, and is related to the general theory of semiclassical approximations to quantum mechanics (see [31], and references therein). In this approach, quantum expectation values are often approximated by statistical averages over a microcanonical ensemble of initial conditions. Several important studies were performed recently in this framework, concerning harmonic generation by a classical hydrogen atom [15], and stabilization in ultrastrong laser fields [32,33].

The second method is derived from the time-dependent variational principle (TDVP) [34]. The wave function is constrained to belong to a particular space of trial functions, defined by a limited number of parameters. The partial differential equations of motion describing the wave function are then replaced by a set of coupled ordinary differential equations, which can have a Hamiltonian form. This method, widely used in nuclear physics, has recently been applied to strong-field atomic physics by Horbatsch and Liakos [35], who studied the motion of an anisotropic Gaussian wave function in a three-dimensional (3D) Coulombic potential, using 12-parameter trial functions. A cruder approximation may be obtained by assuming that the wave function remains a Gaussian of fixed width, and taking as parameters the position expectation value, and its conjugate variable, or "momentum," which can then be shown to follow apparently classical equations of motion. The validity of this kind of classical approximation has been studied in the case of time-independent anharmonic oscillators by Brickmann and Russeger [36] and Gerry [37], and, in the case of the time-dependent Morse oscillator, by Walker and Preston [38]. They conclude that the classical approximation may yield good results, provided few high-lying levels are excited.

It is obviously the second method, based on the TDVP, which is the most appropriate for relating classical and quantum dynamics of the strongly driven anharmonic oscillator. This can be understood simply by considering a driven harmonic oscillator. Its coherent states (Gaussian wave packets minimizing $\Delta x \Delta p$) follow exactly the classical equations of motion; this is due to the fact that the Hamiltonian has the form required to preserve coherence [39,40]. Classical dynamics and quantum dynamics of coherent states are therefore equivalent. This property naturally breaks down when an anharmonic term is introduced in the potential. The purpose of our study is to compare the classical and quantum-mechanical dynamics of the anharmonic oscillator and to understand the differences.

To investigate the quantum-mechanical anharmonic oscillator, we solve numerically the time-dependent Schrödinger equation for the Hamiltonian

$$H = p^2/2 + x^2/2 + v x^4/4 - E_0(t) x \sin(\omega t). \tag{21}$$

The wave function is propagated by a standard three-point Crank-Nicholson algorithm, matrix inversions being performed by the Thomas algorithm. Because of the confining character of the potential, the wave function remains well localized even when the field is strong. The interval to be considered in the computations is therefore much smaller than in the case of Coulomb-type potentials, which allows us both to perform fast computations and to use small space grid size and time implement. We first determine the ground state wave function, by propagating the Schrödinger equation in complex time, starting from a reasonable trial function. This allows us to prevent numerical artifacts due to the different ground states of the continuous and discretized Hamiltonians [11]. The field strength $E_0(t)$ may be considered as slowly time dependent, to account for a smooth turn on of the field. We use either a linear or a $\sin^2$ ramp, typically over five optical cycles or more.

Let us consider first the simple case of an harmonic oscillator. As mentioned before, the expectation value of the position follows the classical equation:

$$\ddot{x} + x = E_0(t) \sin(\omega t). \tag{22}$$

In the case of a sudden turn on of the field, the solution may be written as

$$x(t) = \frac{E_0}{1-\omega^2} [\sin(\omega t) - \omega \sin(t)]. \tag{23}$$

The motion consists of forced oscillations at frequency ω, combined with oscillations at the oscillator frequency $\omega_0 = 1$, corresponding to a solution of the homogeneous part of Eq. (22). Note that the peak amplitude at the unperturbed oscillator frequency $\tilde{x}(\omega_0)$ (with $\omega_0 = 1$) depends on the ramp chosen, and consequently on the whole past of the

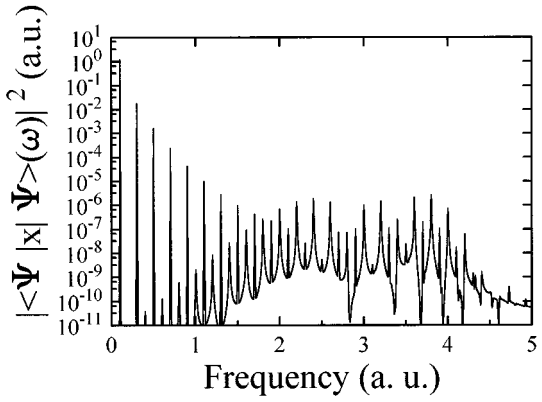

FIG. 4. Spectrum obtained from a quantum-mechanical anharmonic oscillator ($\omega=0.1$, $v=5$, $E_0=8$). The ramp is introduced on 24 optical cycles.

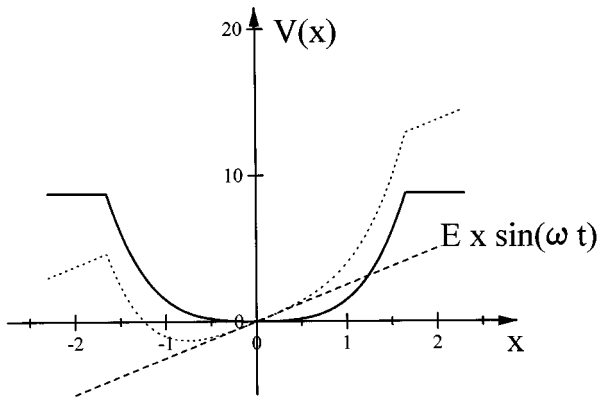

FIG. 5. Anharmonic potential truncated to allow for ionization of the wave function. The dashed line represents the instantaneous potential due to the driving field.

pulse, whereas the ω peak amplitude depends only on the field amplitude E_0 in the steady-state regime.

When a weak anharmonic term is included in the potential, weak and regularly decreasing odd harmonics appear. Moreover, satellite hyper-Raman peaks develop at frequencies $\tilde{\omega}_0 \pm 2p\omega$ around the atomic peak, whose frequency shifts from $\omega_0=1$ to $\tilde{\omega}_0$. New peaks develop as the anharmonic term and the field strength are increased, extending farther away from the $\tilde{\omega}_0$ peak. This phenomenon has also been noticed by Bandarage *et al.* [15] on the classical hydrogen atom, as well as by Taïeb on several types of oscillators [18]. Figure 4 presents a spectrum obtained for $E_0=8$. In order to switch on the driving field adiabatically, we used a $\sin^2$ ramp with 24 optical cycles. The harmonic intensities first decrease steadily with order, then stabilize in a plateau structure. However, the spectrum is blurred by a large number of hyper-Raman peaks, about equal in amplitude to the harmonics. This spectrum is quite similar to that of Fig. 3, obtained in a purely Hamiltonian classical case. Periodicity was then achieved through a small damping term $\Gamma\dot{x}$. It may be worth trying to include an equivalent of this classical damping in the quantum-mechanical system.

Many studies have aimed at obtaining nonconservative quantum-mechanical systems; in particular, the damped harmonic oscillator has drawn much attention.The most relevant scheme consists of coupling the oscillator to an external reservoir [41,42], to which the energy can flow. One possible method in our case is to couple the system to a continuum of electron states, i.e., to include an ionization pathway in the calculation. This is achieved by truncating the potential to a limiting value:

$$V(x)=\frac{x^2}{2}+\frac{v}{4}x^4 \quad \text{for} \quad |x|<|x_l|, \tag{24}$$

$$V(x)=V(x_l)=\frac{x_l^2}{2}+\frac{v}{4}x_l^4 \quad \text{for} \quad x|>|x_l|. \tag{25}$$

The new potential is represented in Fig. 5. Also indicated is the sum of $V(x)$ and the driving term $Ex=E_0x\ \sin(\omega t)$. Clearly, bound states may now be ionized, either by a single-photon (or multiphoton) transition to the continuum, or by tunneling through the barrier. This model is extremely versatile, since the truncation level $V(x_l)$ may be modified to obtain any desired ionization rate, for a given field strength. On the other hand, two numerical difficulties may appear.

The first one originates from possible reflections of the wave function on the grid boundaries [11], which may create spurious harmonic peaks of extremely high order. Several methods exist to absorb the wave function before it reaches any boundary. We chose to use a complex potential, consisting of a linear complex ramp:

$$V(x)=V(x_l)(1+i\alpha|x-x_a|) \quad \text{for} \quad |x|>|x_a|, \tag{26}$$

with $\alpha<0$. The absorbing potential width (from x_a to boundary) and α are chosen so that spurious harmonic peaks disappear. A perfectly rigorous calculation would require $|x_a|$ to be larger than the total excursion $D_{\mathrm{FE}}=2eE/m\omega^2$ of a free electron in the laser field. However, one important characteristic of the anharmonic oscillator is that high-order harmonics are only generated for very large field strengths, of the order of a few atomic units. A free electron excursion in these conditions is several hundred times larger than the width of the potential well. Such a huge grid cannot be considered numerically; we therefore restrict x_a to be of the order of $2x_l$, which implies that any ionized electron is absorbed long before it has a chance to come back to the potential well. Consequently, the semiclassical scenario cannot happen here, and the high harmonics are only due to the oscillator dynamics, and not to field acceleration in the continuum. We checked that the calculated harmonic spectra were independent of the value of x_a ($x_a \ll D_{\mathrm{FE}}$).

The second numerical problem results from the existence of potential singularities at $\pm x_l$. The Crank-Nicholson algorithm is known to be very sensitive to discontinuities in one of the potential derivatives. Indeed, our results depend slightly on the interval between the potential truncation position x_l and the neighboring grid points. However, this does not lead to any loss of generality concerning our analysis: all features of spectra remain unchanged when this interval is varied; only the relative amplitudes and phases of high-order harmonics can be slightly affected. Figure 6(a) shows a typical spectrum obtained at $E_0=10$. A five-cycle linear ramp was used; the TDSE was then propagated over 40 cycles, the Fourier transform being performed over the last eight cycles.

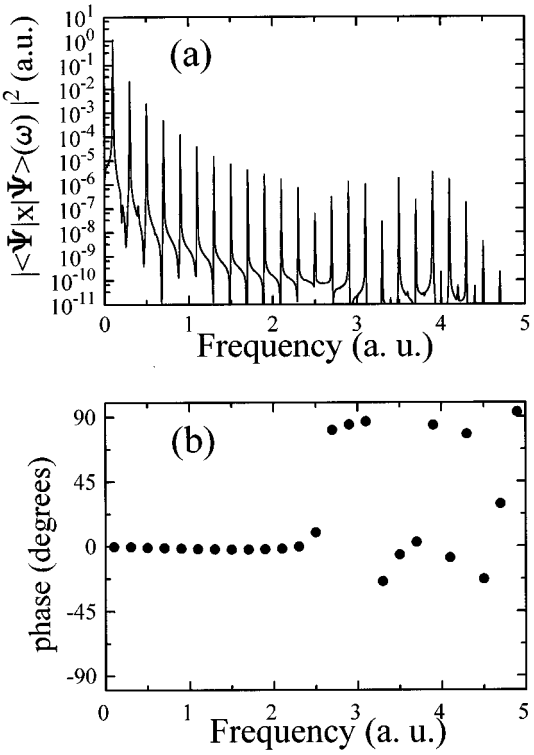

FIG. 6. (a) Spectrum obtained from a truncated anharmonic oscillator [same conditions as in Fig. 1(a), $E_0=10$]. (b) Corresponding phases of the harmonics, relative to the driving field.

The potential truncation value was set so that the potential supports eight metastable excited states when the field reaches its peak value; this was checked with an autocorrelation spectral method [43]. Hyper-Raman peaks have been washed out. As in the classical case, the harmonics plateau is now clear. Note that the background noise is much smaller in these calculations than in most other computer simulations. This noise has been interpreted as due to populated high-lying Rydberg states, which are dipole coupled to the ground state [11]. The confining anharmonic potential presents the peculiar property not to support any Rydberg series of states, since the energy separation between the excited states increases continuously up the continuum threshold imposed by the truncation. As a result, there is no real need to calculate the spectra in the acceleration gauge, or in other more adequate gauges [11].

The parameters used in Fig. 6(a) were chosen to be identical to those of Fig. 1(a). The classical and quantum-mechanical spectra can therefore be compared directly. The general features are obviously similar, with the characteristic decrease, plateau, and cutoff. In particular, the cutoff location follows approximately Eq. (8). This indicates that our classical analysis is still relevant in the quantum case. Several differences are nevertheless clear. In the quantum case, the initial decrease is steeper; moreover, the intensity and extent of the plateau is reduced: it begins at slightly higher frequencies and ends at slightly lower frequencies than in the classical case. These discrepancies can be understood along the lines previously exposed, concerning the validity of classical approximations to quantum mechanics.

We first consider the low-frequency part of the spectrum (initial decrease). We explained previously that the classical case describes the rapid motion of a particle in the slowly varying potential well. The action $\int p_{\delta x} d\,\delta x$ may be arbitrarily small, the trajectory of the electron remaining in the vicinity of the bottom of the well (see Fig. 2). The motion of the latter leads to the low-frequency decreasing part of the spectrum. The quantum case describes the position expectation value of a wave packet. The relevant action is higher, at least of the order of $\hbar/2$ (1/2 in our units) according to the Bohr-Sommerfeld theory. Let us consider one fixed time, for instance when the field is maximum. The outer part of the potential (i.e., the part lowered by the field) is steeper than the inner one (see Fig. 5). This holds, of course, because of the confining anharmonic character of the potential, and would not be true for a harmonic oscillator. As a result, the center of the wave packet is displaced towards the field-free center ($x=0$) as compared to the bottom of the instantaneous well. This would also be true for the average position of a classical trajectory with the same action (the relationship is straightforward in the first classical approximation described previously). This attenuation gets larger when the difference between the softer and the steeper part of the potential gets more pronounced. The low-frequency time variation of the quantum dipole $|d_q|$ is therefore less anharmonic than that of the bottom of the well, so that the first few harmonics display a steeper decrease in the quantum case than in the classical case.

We have interpreted the plateau as due to high-frequency motion in the well. Quantum mechanically, this motion must involve excited states of the adiabatic Hamiltonian. The action of these states is at least of $3\hbar/2$, so that the softening effect just discussed should also occur, and be responsible for the cutoff deviation from Eq. (8). Moreover, the damping term in the classical equations of motion for $x(t)$ was shown to induce a periodic excitation term for $\delta x(t)$ [Eq. (6)]. Though ionization plays the same role in the quantum case, it is not strictly equivalent. As a result, there is actually no reason the intensity level of the high harmonics in the plateau should be exactly the same as in the classical case.

As a whole, what was understood as periodic excitation and damping of high-frequency motion in the classical case should now be viewed as periodic excitation and ionization of excited states of the adiabatic Hamiltonian. The resulting spectra are identical for a harmonic oscillator, but are increasingly different as the anharmonic term becomes stronger. Accounting for these expected limitations, the general qualitative agreement between classical and quantum calculations remains quite remarkable, and indicates that the plateau of harmonics displayed by the strongly driven quantum anharmonic oscillator can largely be understood on a purely classical basis.

IV. DYNAMICAL SINGLE-ATOM PHASE AND COHERENCE EFFECTS

Several unexpected features have been noticed in previous models of high-order harmonic generation that seem to be as characteristic and universal as the plateau-cutoff structure. These features can be observed both in the classical and in the quantum-mechanical anharmonic oscillator models.

A. Intrinsic phases of high-order harmonics

It recently became clear that high harmonics may be completely out of phase from the laser. This was first noticed in the TDSE calculations of Kulander and Schafer, and clarified in the tunneling limit by the model of Lewenstein *et al.* [24]. These relative, or intrinsic, phases actually exist in traditional nonlinear optics: it suffices to introduce a finite lifetime to an intermediate state in the standard perturbative expression for a hyperpolarizability to obtain a complex result. The resulting phase remains, however, small, except in a quasi-resonant situation, and is independent of intensity. In contrast, the intrinsic phases of high harmonics as observed in numerical simulations exist for any laser frequency, and are strongly intensity dependent.

Two major physical issues are related to these intrinsic phases. The first one concerns a possible generation of attosecond pulses of light, by a suitable recombination of selected harmonics. In the Appendix, we detail this idea, and briefly present propagation calculations showing how both intrinsic and propagation-induced phases strongly inhibit the creation of such short pulses. The second issue deals with macroscopic propagation effects for high harmonics. Several authors recently noticed that these intrinsic phases may cause a severe distortion of the harmonic wave front modifying the angular distribution [5,44,45], and may play an important role in the phase-matching process [46].

In the semiclassical model, the intrinsic phases arise from propagation in the continuum: the classical action of motion yields the corresponding phase. A simple heuristic way to understand the origin of those phases is to notice that there is an intensity-dependent time delay between tunnel ionization and return to the ionic core.

The existence of intrinsic phases is also quite clear in the anharmonic oscillator model. Figure 6(b) presents the phases corresponding to the quantum spectrum displayed in Fig. 6(a), and Figs. 7(a)–7(c) those obtained in the conditions of Fig. 1(b). In all cases, the lowest harmonics in the steadily decreasing part of the potential are in phase with the driving field. In contrast, the harmonics of the plateau are out of phase, in an apparently random way. It should be remembered here that the plateau in the classical case starts at lower frequencies (about the 15th harmonic) than in the quantum case.

This behavior can be easily understood along the lines exposed in the first part of this paper. The low harmonics in the decreasing part of the spectrum arise from the low-frequency displacement of the bottom of the well, which is of course perfectly in phase with the laser. The plateau harmonics correspond to rapid motion within the well. There is no *a priori* reason the high- and the low-frequency motion should be in phase.

One may also notice that the damping constant has a major incidence on the phases in the classical case. This is illustrated in Fig. 7, which presents harmonic phases obtained with different damping constants [no damping in Fig. 7(a); weak damping in Fig. 7(b); strong damping in Fig. 7(c)], but otherwise identical conditions. In the purely Hamiltonian case, all phases are almost equal to 0 or 180°; deviations from these two values become significant for weak damping, and there is a significant phase variation from order to order in the case of strong damping. The

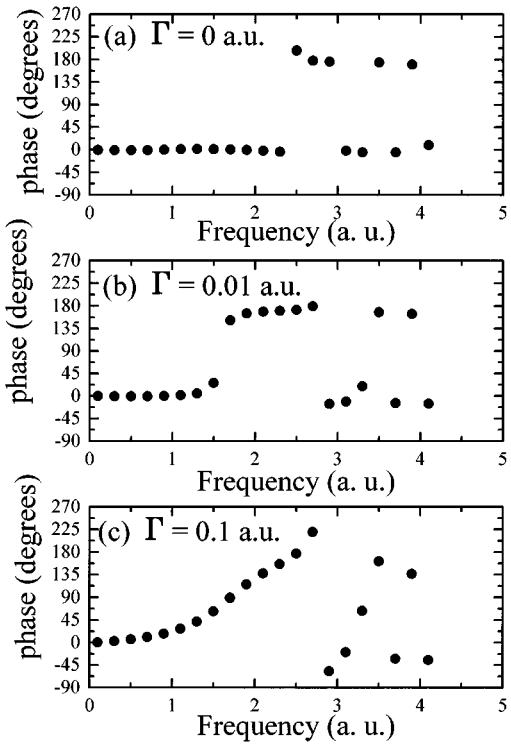

FIG. 7. Intrinsic phases of the harmonics in the conditions of Fig. 1(b), for different damping constants. (a) no damping; (b) weak damping; (c) strong damping.

phases shown in Fig. 7(c) actually display a rather regular behavior. At the transition between the decrease and the plateau, they follow approximately a quadratic dependence on the harmonic frequency.

These features can be demonstrated using simple recurrence relations between the harmonic amplitudes d_q [27]. Assuming that the motion is periodic,

$$d(t)=\sum_{-\infty}^{+\infty} d_q e^{iq\omega t}, \tag{27}$$

and considering that the strongest harmonic peak is by far that at the fundamental frequency, then one gets the simple recurrence relation

$$d_{q-2}+d_{q+2}=\left(2+4\frac{\omega_0^2+iq\Gamma-q^2\omega^2}{3vd_1^2}\right)d_q. \tag{28}$$

When $\Gamma=0$, this recurrence remains in the real domain, and the only allowed phases are 0 and π. When $\Gamma\neq 0$, then the phases between the harmonics at the beginning of the plateau are related to first order by

$$\arg(d_{q+2})-2\arg(d_q)+\arg(d_{q-2})=\frac{4q\Gamma}{3vd_1^2}, \tag{29}$$

which explains the approximately quadratic behavior observed in Fig. 7(c). Note that this method is very close to that proposed by Plaja and Roso-Franco [17] and Kaplan and Shkolnikov [19].

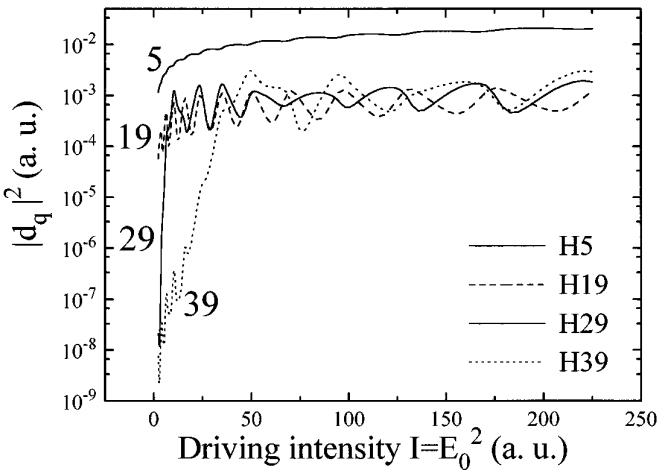

FIG. 8. Intensity dependences of the harmonic intensity $|d_q|^2$, for harmonics 5, 19, 29, 39, in the classical anharmonic oscillator.

In conclusion, the anharmonic oscillator model explains simply why the plateau harmonics (and only those) are out of phase with the laser. In a purely Hamiltonian, or weak damping, situation, the harmonics can only have phases close to 0 or π. In all models (perturbation theory, semiclassical model, anharmonic oscillator), the intrinsic phases may get arbitrary values when a strong coupling to a continuum is introduced, even in nonresonant conditions.

B. Interference effects

We now examine the dependence of harmonic amplitudes as a function of intensity. We focus here on the analysis of the classical case.

Equation (20) implies that the motion at time t results from a linear superposition of oscillations, excited previously over a time range of the order of $1/\Gamma$. The Fourier component d_q of the dipole at frequency $q\omega$ can therefore also be analyzed as a sum of components excited at different times, and consequently modulated by phase factors $\exp(-iq\omega\Delta t)$ (Δt denoting the time between two excitations). If any parameter of the problem is changed, then the relative weights of these components should vary, so that one may expect interference effects to occur. As an example, Fig. 8 presents the intensity ($I=E_0^2$) dependence of $|d_q|^2$ for harmonics 5, 19, 29, and 39. The curves indeed display very clear oscillations. A simple way to check our interpretation consists in increasing the damping term Γ to values larger than ω, thus limiting the excitation duration to less than an optical period; in such conditions, interference effects are bound to be dramatically reduced. Numerical tests show that all oscillations are indeed washed out.

These results can be compared with those from other studies. It seems that all quantum models for high-order harmonic generation yield this kind of oscillations. They are particularly clear in the work of Krause, Schafer, and Kulander [11], and were even shown to exist experimentally [47]. In the tunneling regime for the atomic response [24], these oscillations were interpreted as interferences between electron wave functions following different classical trajectories. Note, however, that such oscillations already exist in a multiphoton regime. A similar behavior has also been predicted by Kaplan and Shkolnikov in a two-level system [19]. The previous arguments do not imply, however, that all structures can only be due to interferences; the Floquet calculations of Smith and Potvliege [49] indeed show very clearly both multiphoton resonances, appearing as series of sharp peaks when atomic states come into resonance, and broader interference oscillations. It can be shown by simple analytical arguments [48] that thin spatial structures in the medium polarization, such as those due to multiphoton resonances, do not survive phase matching. Steplike patterns observed in experimental intensity dependences [47] may therefore be due to these (broad) interference effects. However, this would deserve a more detailed theoretical study, including both single-atom response and propagation, which goes beyond the scope of the present paper.

It may seem puzzling that a simple *classical* model should predict an effect analogous to *quantum-mechanical* interferences. This essentially stems from the fact that the anharmonic oscillator nonlinear equations could be replaced in the adiabatic approximation by linear equations, describing a time-dependent harmonic oscillator. This linearity allows us to make use of the superposition principle, just as in quantum mechanics.

The difference between the cutoff and plateau regions, for a given harmonic, is particularly clear in this model: the harmonic first increases very steeply, up to the intensity at which the cutoff, given by Eq. (8), reaches the harmonic frequency (or, in other words, at which the harmonic reaches the plateau region). Then, the harmonic increases rather slowly ($|d_q|\sim|E_0|^{1/3}$). Once again, this feature seems to be present in any model of high-order harmonic generation, and was demonstrated experimentally [8]. Remarkably, the essential characteristics of high-order harmonic generation by real atoms can be reproduced and explained in this extremely simple, almost naive, model of a classical anharmonic oscillator.

C. Dynamical coherence effects

In this last part, we would like to come back to our previous discussion on the importance of damping and ionization, as well as the presence of hyper-Raman peaks in the absence of these relaxation processes. It could be argued that these additional peaks are of no importance to high harmonics, since the frequencies are different anyway. We wish to emphasize that the existence of these spurious peaks is symptomatic of a coherence problem for the high harmonics.

One sometimes considers that hyper-Raman peaks can be prevented by an extremely gradual, fully adiabatic, switch on of the forcing field, without having to take relaxation processes into account. In the important example of the harmonic oscillator, simple analytical calculations show that the intensity of the ''atomic'' peak indeed tends to zero as the ramp duration tends to infinity. We performed a thorough series of attempts to switch on the forcing field very gradually, on several tens of optical cycles. We were unable to obtain pure harmonic spectra without introducing relaxation into the model. In all cases, the resulting spectrum displays hyper-Raman peaks. Their intensity is high for very short ramps (almost sudden turn on of the field), as well as for

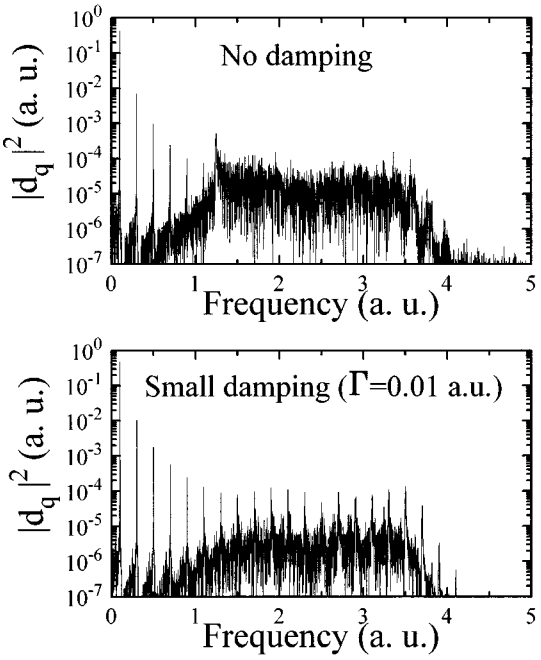

FIG. 9. Classical spectrum obtained from a realistic Gaussian pulse (full width at half maximum of 128 optical cycles), (a) without damping, and (b) in weak damping conditions ($\Gamma=0.01$).

very long ramps. The ramp duration in Fig. 4 was actually chosen in order to minimize the intensity of these peaks.

The dependence of the hyper-Raman peaks on the length of the ramp can be understood on simple grounds, both in the classical and the quantum case. In the classical case, Eq. (20) shows that the motion depends on the previous values of the field on a time interval of the order of $1/\Gamma$. If the damping constant is set to zero, then the motion depends on the whole past of the pulse, including turn on. In the quantum case, the hyper-Raman peaks were interpreted by Taïeb [18] and by Millack and Maquet [50] as frequency beats between the ground Floquet state and one of the higher Floquet states. The quasienergies are intensity dependent, and therefore so are the hyper-Raman frequencies. The excited Floquet state can be populated by an avoided crossing in the course of the field turn on [51], which explains that these hyper-Raman peaks actually increase when the ramp is too long.

In Fig. 9, we show two spectra calculated in the classical case, using a realistic pulse envelope:

$$E(t)=E_0\sin(\omega t)\sin^2\left(\frac{2t}{T_p}\right), \tag{30}$$

where $T_p=128(2\pi/\omega)$ denotes the pulse duration at half intensity. The Fourier transform is performed over the entire pulse. No damping is considered in Fig. 9(a), whereas a weak damping ($\Gamma=0.01$) was introduced in the calculation for Fig. 9(b). Both spectra are much noisier than with the standard procedure, consisting of a ramp and a constant field plateau, which explains why the former method has been rarely used in the numerical calculations of high-order harmonics [13,52]. In Fig. 9(a), the plateau harmonics are completely swallowed in a very large background noise, which we may interpret as a superposition of hyper-Raman peaks of frequencies varying with intensity during the pulse. On the other hand, harmonics can clearly be distinguished in Fig. 9(b), in spite of a still important background. Other, more rigorous, methods used to compute the emission spectra also yield hyper-Raman and/or background noise [53].

We have shown how the hyper-Raman peaks depend critically on how the field is switched on. One may wonder if (or in which conditions) the harmonics themselves are affected by the characteristics of the field turn on. To understand this, we have performed systematic calculations, in the classical case, using the standard method where the field is switched on by a ramp and subsequently held fixed. The harmonics were calculated right after the end of the ramp, for different ramp durations. The first harmonics, which correspond to the initial decrease in the spectrum, do not depend on the ramp shape or duration. This seems logical, since these harmonics are interpreted as the Fourier components of the motion of the bottom of the potential well, which depends only on the instantaneous field intensity. The intensities and phases of the plateau harmonics appear to be highly sensitive to the ramp parameters when the duration of the ramp is less than $1/\Gamma$. They are, however, independent of the turn-on parameters for longer ramp durations. This shows that it does not really make sense to compute a harmonic spectrum for extremely weak damping, for which $1/\Gamma>T_p$. As shown in Sec. II, the high-frequency motion is due to oscillations excited over a time range of $1/\Gamma$. It seems therefore inevitable that the system requires times of the order of $1/\Gamma$ to adapt to any field variation and reach a stationary state, resulting in a converged value for the harmonic complex amplitude.

Similar results are also obtained in the quantum-mechanical case, and can be interpreted along the line proposed in [50], using a Floquet analysis. Let $\Phi_1(t)$ be the ground Floquet state and $\Phi_2(t)$ another Floquet state with quasienergies and widths E_1, γ_1 and E_2, γ_2, respectively. The wave function reads

$$\Psi(t)=c_1e^{-i(E_1-i\gamma_1)t}\Phi_1(t)+c_2e^{-i(E_2-i\gamma_2)t}\Phi_2(t), \tag{31}$$

which yields the dipole moment

$$\begin{aligned}\mathbf{d}(\mathbf{t})=&|c_1|^2e^{-2\gamma_1t}\langle\Phi_1(t)|\mathbf{d}|\Phi_1(t)\rangle\\&+|c_2|^2e^{-2\gamma_2t}\langle\Phi_2(t)|\mathbf{d}|\Phi_2(t)\rangle\\&+2e^{-(\gamma_1+\gamma_2)t}\mathrm{Re}[c_1c_2^*e^{-i(E_1-E_2)t}\langle\Phi_1(t)|\mathbf{d}|\Phi_2(t)\rangle].\end{aligned} \tag{32}$$

Since $\Phi_1(t)$ and $\Phi_2(t)$ are periodic, the first two terms in the right-hand side in Eq. (32) contain the harmonics, whereas the cross terms yield the hyper-Raman lines. The occurrence of such lines in harmonic spectra means therefore that at least one excited Floquet state was populated by an avoided crossing during the field turn on. The periodic part of $d(t)$ then consists of the contribution of the ground Floquet state $\Phi_1(t)$, plus that of $\Phi_2(t)$ which decays on a time scale of $1/\gamma_2$. This implies that converged (i.e., turn-on independent) harmonics cannot be obtained before the system has relaxed to its ground Floquet state, i.e., when the hyper-Raman lines have disappeared. We are therefore led to introduce a new

characteristic time T_d, which corresponds essentially to the decay time of the Floquet state Φ_2. One usually has

$$T_L < T_d \ll T_p, \tag{33}$$

where $T_L = 2\pi/\omega$ is the optical cycle duration, and T_p denotes again the pulse duration. In that case the *temporal locality* holds, in the sense that the atomic polarization follows ''instantaneously'' the laser field excitation, with the usual coherence properties. However, one might consider cases for which

$$T_L \ll T_p \simeq T_d. \tag{34}$$

In this case, the coherence properties of the harmonic emission may be deteriorated. Indeed, atoms located at different places in the focal volume may be submitted, at one time, to the same local intensity, but with different (local) past history of the laser field. This results in different populations for the Floquet states, and hence different amplitudes and phases for the harmonic emission [see Eq. (32)]. A rigorous study of coherence effects induced by the breakdown of the temporal locality is far beyond the scope of the present paper: it would actually require simultaneously solving the TDSE for all points in the focal volume and the Maxwell equations of propagation. Some attempts have nevertheless already been performed in that direction [54].

These considerations explain simply why the harmonic amplitudes are usually computed *after* the hyper-Raman peaks have decayed. It is also worthwhile to notice that ionization, which is usually considered as a competing process to high-harmonic generation, actually plays an important role in the high-harmonic generation process, by rapidly depleting the excited Floquet states in a dynamical regime, thus granting the coherence of high harmonics in most realistic situations.

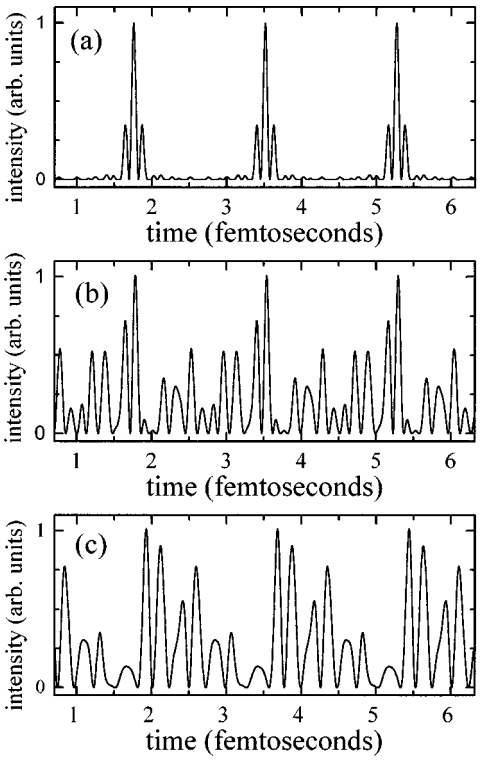

FIG. 10. Intensity of the electric field corresponding to the coherent sum of harmonics 7–21 in xenon irradiated by 1.06 μm laser light. (a) assuming constant phases and amplitudes; (b) taking into account realistic single-atom dipole moments (see text); (c) including propagation effects.

V. CONCLUSION

We have proposed in this paper a detailed analysis of high-order harmonic generation in strongly driven Duffing oscillators, from both classical and quantum-mechanical point of view. Our primary purpose was to determine the conditions for which high harmonics arise, and to unravel their origin.

Classically, we have shown that the low-frequency character of the driving field allows analysis of the motion by means of the adiabatic invariance theorem. Two time scales can indeed be distinguished, one associated to the low-frequency displacement of the bottom of the well, and the other to the high-frequency motion within the well. This duality results in a splitting of the harmonic spectrum into two regions, namely, the initial decrease and the plateau. The cutoff appears naturally as the highest characteristic frequency of the potential, modified by a strong quasistatic field. This kind of scaling is very close to that proposed by Bandarage *et al.* [15] for the classical hydrogen atom. We pointed out that a small damping term should be introduced, so that the motion may relax to a stable periodic orbit.

Quantum mechanically, we have demonstrated that a pure harmonic spectrum can also be obtained, provided an ionization pathway is allowed. General features of the quantum spectrum were shown to be similar to those of the classical one. Differences arising from the quantum nature of the model, due to deviation from the harmonic oscillator case, were nevertheless observed and analyzed. Our analysis also explains why the plateau harmonic peaks and the hyper-Raman peaks always span the same frequency range. This point still stimulates theoretical interest [55].

The very simplicity of the model makes it possible to discuss a number of other characteristic properties of high-order harmonics. In particular, we show how intrinsic phases and interference effects arise in the model. Finally, we emphasize that high-order harmonic generation is a dynamical process, whose response time T_d is linked to the ionization process.

Finally, we would like to stress that the present model could profitably be used for pedagogical purposes. It is indeed quite remarkable that the same simple model that usually helps students to understand the basics of nonlinear optics (second- and third-order harmonic generation) can also be used to illustrate and get important insights into the physics of high-order harmonic generation, which is one of the latest and most striking ''exotic'' phenomena in atomic and optical physics.

ACKNOWLEDGMENTS

We would like to thank K. C. Kulander, M. Lewenstein, A. Maquet, D. Richards, P. Salières, and K. J. Schafer for numerous and fruitful discussions. We also thank K. C. Ku-

lander and K. J. Schafer for providing the single-atom data used in the calculations of the Appendix.

APPENDIX A

A recurrent theme concerns the possibility of using high harmonics to generate extremely short pulses of light. Several physicists have indeed noticed that the characteristic plateau of high harmonics is very similar to the spectrum of a mode-locked multimode laser [56], or of phase-locked laser oscillators [57], and suggested therefore the following idea. Suppose one is able to get rid of the first few harmonics (decreasing part of the spectrum), and of the last ones (cutoff region), and to keep only the plateau harmonics through selection by adequate filters. If the harmonics are all in phase, then the addition of the electric fields would lead to a train of ultrashort pulses, separated by one half period of the fundamental. The duration of each pulse is given by the inverse of the frequency range of the selected harmonics:

$$\tau_{\text{pulse}} \simeq \frac{1}{(\omega_{\max} - \omega_{\min})}. \tag{A1}$$

Let us consider as an example the case of a xenon atom irradiated by 1.06 μm laser light. We show in Fig. 10(a) the temporal structure resulting from the addition of the seventh to 21st harmonics, assumed to have equal amplitudes and phases. The pulse duration derived from Eq. (A1) is approximately equal to 40 attoseconds.

However, this attractive idea relies on the assumption that all the harmonics have the same phase. Figure 10(b) shows the result of a calculation adding the harmonic field complex amplitudes (from the seventh to the 21st) at 5×10^{13} W cm^{-2} for a single xenon atom, obtained by solving the time-dependent Schrödinger equation [10]. The regularity displayed in Fig. 10(a) has disappeared: the well-defined pulses have split into more numerous sharp temporal structures. If one includes also the effect of propagation in a thin nonlinear medium [9], then these structures broaden, as illustrated in Fig. 10(c). In this case, i.e., at a relatively low laser intensity, in the ''multiphoton'' regime, the plateau does not behave as a mode-locked laser, but rather as a multimode laser, with sharp and indeed very short substructures. One might speculate on the possibility of selecting an appropriate number of harmonics (approximately in phase) or to bring them back in phase. A more detailed investigation of this problem for harmonic generation in the tunneling regime will be presented elsewhere [59]. It should be stressed that this scheme to generate *trains* of subfemtosecond pulses should not be confused with an idea recently proposed by Ivanov *et al.* [58] that uses the large sensitivity of the high-harmonic generation efficiency to the laser field degree of elliptical polarization to produce a single attosecond pulse.

[1] A. L'Huillier and Ph. Balcou, Phys. Rev. Lett. **70**, 774 (1993).

[2] J. J. Macklin, J. D. Kmetec, and C. L. Gordon III, Phys. Rev. Lett. **70**, 766 (1993).

[3] Ph. Balcou, P. Salières, K. S. Budil, T. Ditmire, M. Perry, and A. L'Huillier, Z. Phys. D **34**, 107 (1995).

[4] J. W. G. Tisch, R. A. Smith, J. E. Muffett, M. Ciarroca, J. P. Marangos, and M. H. R. Hutchinson, Phys. Rev. A **49**, R28 (1994).

[5] J. Peatross and D. D. Meyerhofer, Phys. Rev. A **51**, R906 (1995).

[6] P. Salières, T. Ditmire, K. S. Budil, M. D. Perry, and A. L'Huillier, J. Phys. B **27**, L217 (1994).

[7] M. E. Faldon, M. H. R. Hutchinson, J. P. Marangos, J. E. Muffett, R. A. Smith, J. W. G. Tisch, and C.-G. Wahlstrom, J. Opt. Soc. Am. B **9**, 2094 (1992); T. Starczewski, J. Larsson, C.-G. Wahlström, J. W. G. Tisch, R. A. Smith, J. E. Muffett, and M. H. R. Hutchinson, J. Phys. B **27**, 3291 (1994).

[8] C.-G. Wahlström, J. Larsson, A. Persson, T. Starczewski, S. Svanberg, P. Salières, Ph. Balcou, and A. L'Huillier, Phys. Rev. A **48**, 4709 (1993).

[9] A. L'Huillier, L. A. Lompré, G. Mainfray, and C. Manus, in *Atoms in Intense Radiation Fields*, Advances in Atomic, Molecular, and Optical Physics, Suppl. 1, edited by M. Gavrila (Academic Press, New York, 1992).

[10] K. C. Kulander, K. J. Schafer, and J. F. Krause, in *Atoms in Intense Radiation Fields*, Advances in Atomic, Molecular, and Optical Physics, Suppl. 1, edited by M. Gavrila (Academic Press, New York, 1992).

[11] J. L. Krause, K.J. Schafer, and K.C. Kulander, Phys. Rev. A **45**, 4998 (1992).

[12] R. M. Potvliege and R. Shakeshaft, Phys. Rev. A **40**, 3061 (1989).

[13] J. H. Eberly, Q. Su, and J. Javanainen, Phys. Rev. Lett. **62**, 881 (1989).

[14] V. C. Reed and K. Burnett, Phys. Rev. A **46**, 424 (1992).

[15] G. Bandarage, A. Maquet, T. Ménis, R. Taïeb, V. Véniard, and J. Cooper, Phys. Rev. A **46**, 380 (1992).

[16] B. Sundaram and P. W. Milonni, Phys. Rev. A **41**, 6571 (1990).

[17] L. Plaja and L. Roso-Franco, J. Opt. Soc. Am. B **9**, 2210 (1992).

[18] R. Taïeb, thèse de doctorat, Université Pierre et Marie Curie, 1993 (unpublished).

[19] A. E. Kaplan and P. L. Shkolnikov, Phys. Rev. A **49**, 1275 (1994).

[20] J. L. Krause, K. J. Schafer, and K. C. Kulander, Phys. Rev. Lett. **68**, 3535 (1992).

[21] K. C. Kulander, K. J. Schafer, and J. L. Krause, in *Proceedings of the Super-Intense Laser-Atom Physics III Workshop*, Vol. 316 of *NATO Advanced Study Institute, Series B: Physics*, edited by B. Piraux (Plenum Press, New York, 1993).

[22] P. B. Corkum, Phys. Rev. Lett. **71**, 1994 (1993).

[23] A. L'Huillier, M. Lewenstein, P. Salières, Ph. Balcou, M. Ivanov, J. Larsson, and C.-G. Wahlström, Phys. Rev. A **48**, R3433 (1993).

[24] M. Lewenstein, Ph. Balcou, M. Y. Ivanov, A. L'Huillier, and P. Corkum, Phys. Rev. A **49**, 2117 (1994).

[25] N. Bloembergen, *Introduction to Non-Linear Optics* (Benjamin, New York, 1965).

[26] Y. R. Shen, *The Principles of Non-Linear Optics* (Wiley-Interscience, New York, 1984).

[27] A. L'Huillier, Ph. Balcou, K. J. Schafer, and K. C. Kulander, in *Coherence Phenomena in Atoms and Molecules*, NATO Workshop, edited by A. D. Bandrauk and A. C. Wallace (Plenum Press, New York, 1991).
[28] A. Nayfeh and M. Mook, *Nonlinear Oscillations* (Wiley, New York, 1979).
[29] S. K. Bose, U. B. Dubey, and N. Varna, Fortschr. Phys. **37**, 761 (1989).
[30] W. S. Loud, J. Math. Phys. **34**, 173 (1955).
[31] M. C. Gutzwiller, *Chaos in Classical and Quantum Mechanics* (Springer-Verlag, New York, 1990).
[32] F. Benvenuto, G. Casati, and D. L. Shepelyanski, Phys. Rev. A **45**, 7670 (1992).
[33] M. Gajda, J. Grochmalicki, M. Lewenstein, and K. Rzazewski, Phys. Rev. A **46**, 1638 (1992).
[34] P. Kramer and M. Saraceno, in *Geometry of the Time-Dependent Variational Principle in Quantum Mechanics*, edited by J. Ehlers, K. Hepp, R. Kippenhahn, H. A. Weidenmüller, and J. Z. Hartz, Lecture Notes in Physics Vol. 140 (Springer-Verlag, Berlin, 1981).
[35] M. Horbatsch and J.K. Liakos, Phys. Rev. A **45**, 2019 (1992).
[36] J. Brickmann and P. Russeger, J. Chem. Phys **75**, 5744 (1981).
[37] C. C. Gerry, Phys. Lett. A **146**, 363 (1990).
[38] R. B. Walker and R. K. Preston, J. Chem. Phys. **67**, 2017 (1977).
[39] R. J. Glauber, Phys. Lett. **21**, 650 (1966).
[40] D. Stoler, Phys. Rev. **11**, 3033 (1975).
[41] R. Benguria and M. Kac, Phys. Rev. Lett. **46**, 1 (1981).
[42] C. Cohen-Tannoudji, J. Dupont-Roc, and G. Grynberg, *Processus d'Interaction entre Photons et Atomes* (CNRS-interéditions, Paris, 1988).
[43] M. D. Feit, J. A. Fleck, Jr., and A. Steiger, J. Comput. Phys. **47**, 412 (1982).
[44] J. Muffett, C.-G. Wahlström, and M. H. Hutchinson, J. Phys. B **27**, 5693 (1994).
[45] J. Peatross, M. V. Fedorov, and K. C. Kulander, J. Opt. Soc. Am. B **12**, 863 (1995).
[46] P. Salières, Anne L'Huillier, and M. Lewenstein, Phys. Rev. Lett. **75**, 3776 (1995).
[47] Ph. Balcou and A. L'Huillier, Phys. Rev. A **47**, 1447 (1993).
[48] Ph. Balcou, thèse de doctorat, Université Pierre et Marie Curie, 1993 (unpublished).
[49] P. Smith and R. M. Potvliege, in *Proceedings of the Super-Intense Laser-Atom Physics III Workshop*, Vol. 316 of *NATO Advanced Study Institute, Series B: Physics*, edited by B. Piraux (Plenum Press, New York, 1993).
[50] T. Millack and A. Maquet, J. Mod. Opt. **40**, 2161 (1993).
[51] T. Millack, in *Proceedings of the Super-Intense Laser-Atom Physics III Workshop*, Vol 316 of *NATO Advanced Study Institute, Series B: Physics* (Ref. [21]).
[52] S. C. Rae, X. Chen, and K. Burnett, Phys. Rev. A **50**, 1946 (1994).
[53] F. I. Gauthey, C. H. Keitel, P. L. Knight, and A. Maquet, Phys. Rev. A **52**, 525 (1995).
[54] K. Burnett and S. C. Rae, in *Proceedings of the Super-Intense Laser-Atom Physics III Workshop*, Vol. 316 of *NATO Advanced Study Institute Series B: Physics* (Ref. [21]).
[55] G. Compagno, K. Dietz, and F. Persico, J. Phys. B **92**, 4779 (1994).
[56] S. E. Harris, J. J. Macklin, and T. W. Hänsch, Opt. Commun. **100**, 487 (1993); G. Farkas and C. Toth, Phys. Lett. A **168**, 447 (1992).
[57] T. W. Hänsch, Opt. Commun. **92**, 71 (1990).
[58] M. Yu. Ivanov, P. B. Corkum, T. Zuo, and A. Bandrauk, Phys. Rev. Lett. **75**, 2933 (1995).
[59] P. Antoine, A. L'Huillier, and M. Lewenstein (private communication).